

Hydrogeology Journal – electronic supplementary material

Estimating aquifer recharge in fractured hard rock: analysis of the methodological challenges and application to obtain a water balance (Jaisamand Lake Basin, India)

Melissa M. Rohde^{1*}, W. Mike Edmunds², David Freyberg¹, Om Prakash Sharma³, Anupma Sharma⁴

1. Department of Civil and Environmental Engineering, Stanford University, Stanford, California, USA
2. School of Geography and Environment, University of Oxford, Oxford, England
3. Wells for India, Udaipur, Rajasthan, India
4. National Institute of Hydrology, Roorkee, Uttarakhand, India

*Corresponding Author Address:

Jerry Yang & Akiko Yamazaki Environment & Energy Building

Stanford University

473 Via Ortega

Stanford, California 94305 USA

melrohde@gmail.com

Tel: 650-468-1901

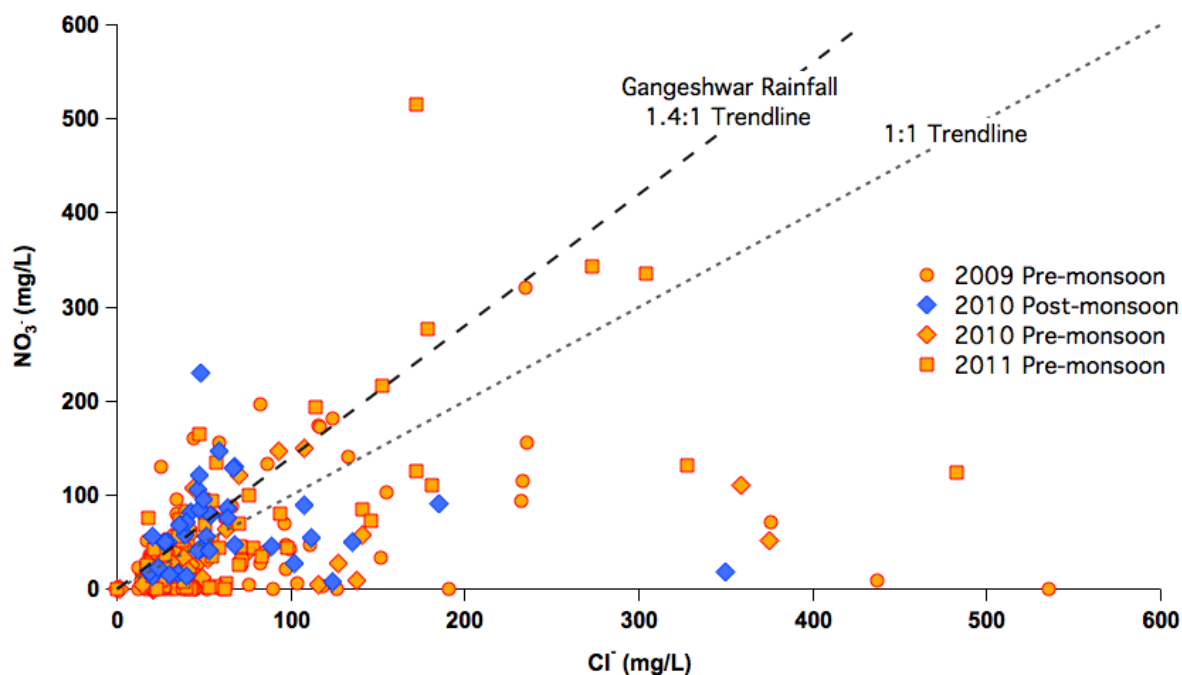
1. Ancillary chemical analysis

Fluoride: Primary geogenic Cl^- may be present in biotite and other layer-lattice minerals (Kamineni 1987). However, in the deeply weathered basement rocks in Rajasthan any primary Cl^- in biotite would have been lost through alteration and unlikely to contribute to shallow groundwater. Deep ancient groundwater in granitic rocks (below present-day active circulation) commonly contains Cl^- which could have accumulated from various sources according to past geological and climatic conditions (Fritz and Frapé 1987). Fluoride is more widely present in primary minerals of the more basic igneous rocks, including biotite and hornblende, and release F^- progressively due to weathering (Edmunds and Smedley 2013). The presence of F^- in groundwater therefore is of geogenic origin and can be used as a proxy to investigate the potential contamination of Cl^- in groundwater from older water. Fluoride is present in most natural waters at concentrations less than 1.0 mg/L (Hem 1985). Fluoride was detected in only 60 % of the samples throughout the Gangeshwar watershed with 5.4 % of the samples containing F^- concentrations greater than 1.0 mg/L. Fluoride concentrations from each pre-monsoon sampling period reached a maximum of 1.9 mg/L in 2009, 1.3 mg/L in 2010, and 1.0 mg/L in 2011. The 2010 post-monsoon F^- concentrations were higher in general, accounting for 2.5 % of all the collected samples with F^- concentrations greater than 1.0 mg/L and a maximum concentration of 2.4 mg/L. Despite the fact that F^- contamination is endemic to the granitic terrain of Rajasthan (Choubisa 2001) due to prolonged water-rock interactions, these low F^- concentrations suggest a short residence time of groundwater and negligible geogenic contribution of Cl^- in the Gangeshwar.

Nitrate: Anthropogenic contributions of Cl^- in groundwater can also derive from agricultural activities, such as the application of fertilizers. The relationships between NO_3^- and Cl^- from the 2009-2011 groundwater dataset are plotted in Fig. S1 with a reference 1:1 trendline and a trendline that characterizes the NO_3^- and Cl^- relationship in the 2010 Gangeshwar rainfall samples. NO_3^- in rain is terrestrially derived possibly due to the release of NO_3^- from biomass burning or forest fires (Edmunds et al. 2002). The accumulation of NO_3^- in groundwater in excess to the Gangeshwar rainfall trendline is likely to be naturally sourced by nitrogen-fixing crops (i.e. chickpeas, groundnuts, soybeans), and/or anthropogenically sourced from the application of inorganic and organic fertilizers. The majority of groundwater samples fall under the 1.4-weighted average Gangeshwar-rainfall NO_3^- and Cl^-

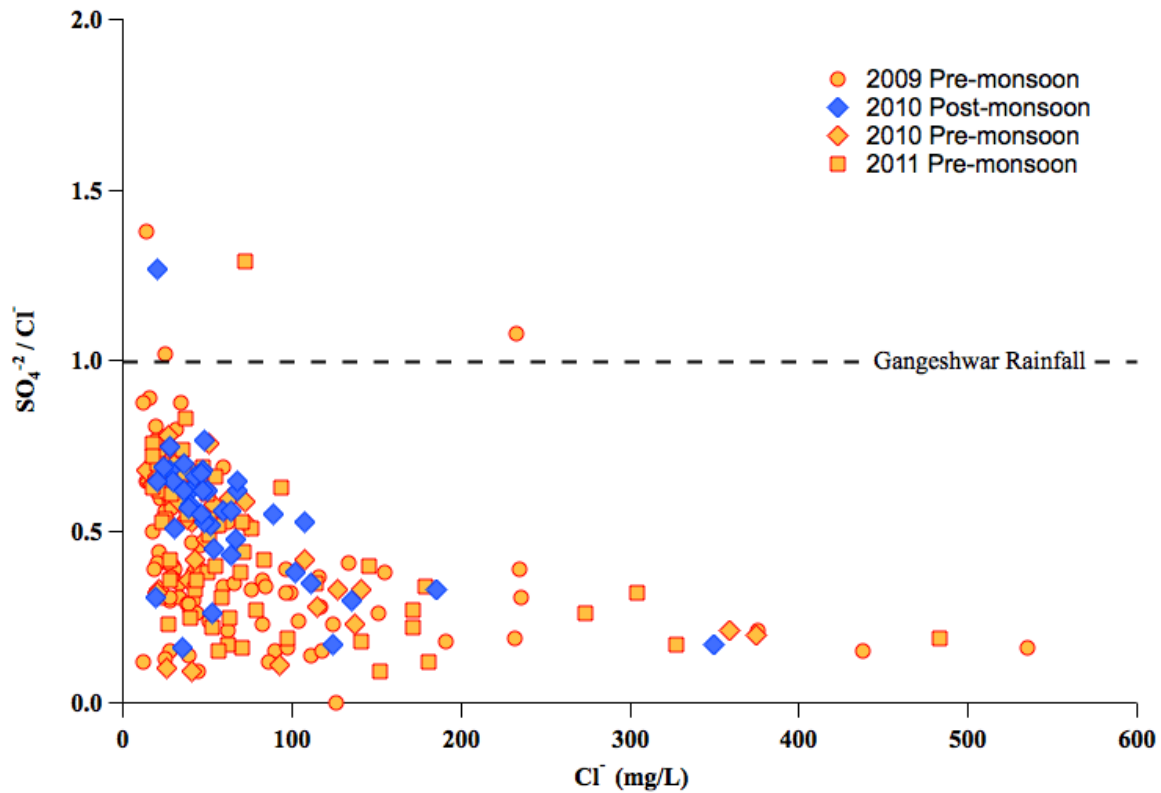
trendline. The depletion of NO_3^- relative to Cl^- in these groundwater points is likely reflecting the high NO_3^- uptake by plants and/or large relative evaporation losses during flood irrigation that result in a high accumulation of Cl^- in the pre-monsoon samples. Anthropogenic inputs of Cl^- from agriculture in this study are assumed to be negligible, since the majority of the samples fall below the Gangeshwar rainfall trendline.

Fig. S1 NO_3^- and Cl^- concentrations in groundwater samples, 2009-2011.



Sulphate: Comparing the $\text{SO}_4^{2-}/\text{Cl}^-$ mass ratios relative to Cl^- in groundwater versus local rainfall can further validate the assumption that atmospheric deposition is the only source of Cl^- in groundwater. The weighted $\text{SO}_4^{2-}/\text{Cl}^-$ ratio of rainfall in the Gangeshwar is 1.0. At low salinities, $\text{SO}_4^{2-}/\text{Cl}^-$ varies considerably and the majority of the $\text{SO}_4^{2-}/\text{Cl}^-$ ratios in the 2009-2011 samples are lower than the weighted $\text{SO}_4^{2-}/\text{Cl}^-$ ratio of the Gangeshwar rainfall (Fig. S2). This suggests that if one assumes Cl^- is conservative, SO_4^{2-} is derived mainly from precipitation and that the variation would be due to the uptake of SO_4^{2-} . Uptake of SO_4^{2-} by local crops and native plants is most likely to account for the observed variability. The groundwater samples with a larger $\text{SO}_4^{2-}/\text{Cl}^-$ ratio of 1.0 are minimal. The lower $\text{SO}_4^{2-}/\text{Cl}^-$ ratios in groundwater relative to the weighted Gangeshwar rainfall ratio of 1.0 contribute additional evidence that Cl^- is sourced by atmospheric deposition.

Fig. S2 $\text{SO}_4^{2-}/\text{Cl}^-$ versus Cl^- concentrations in groundwater, 2009-2011.

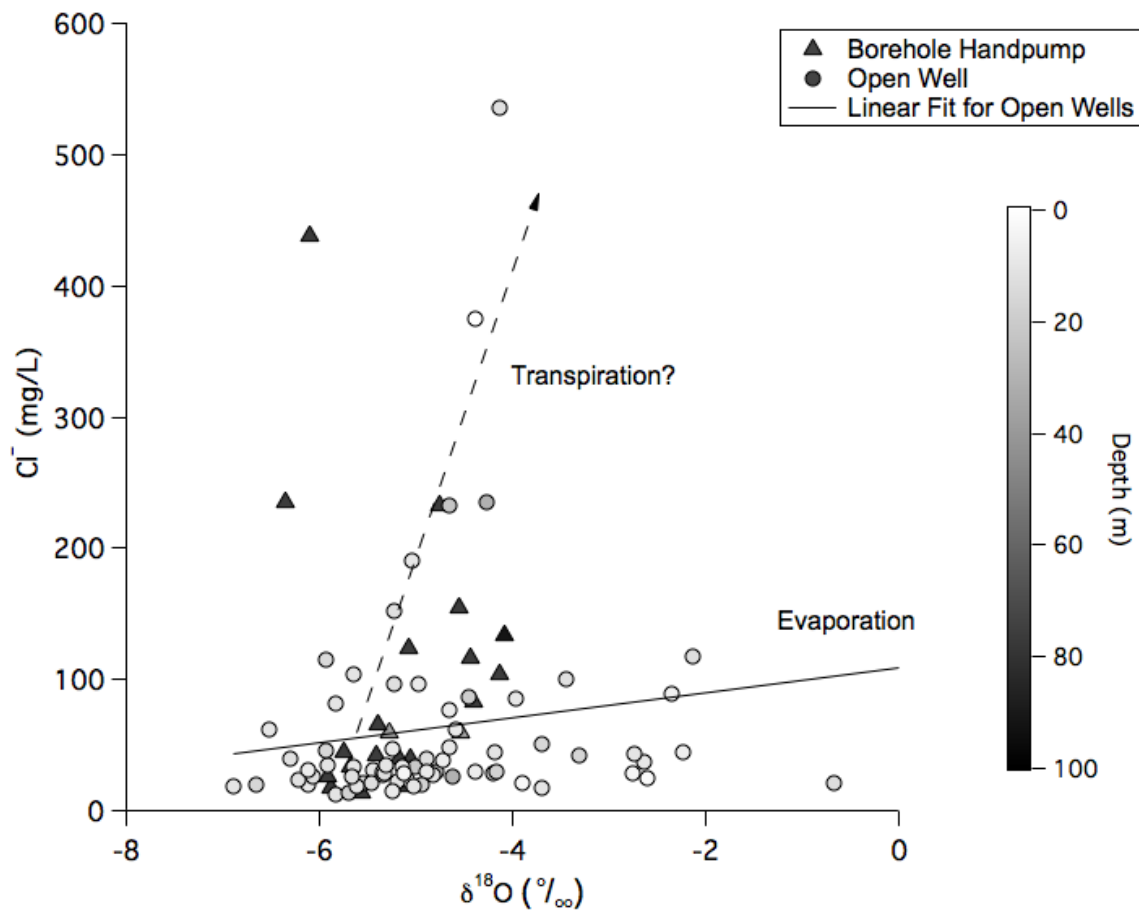


2. Evapotranspiration and irrigated return flow

Differences in the enrichment of Cl^- , $\delta^2\text{H}$, and $\delta^{18}\text{O}$ during evaporation and transpiration allow these two processes to be discerned separately in the isotope water balance. Isotope fractionation of $\delta^2\text{H}$ and $\delta^{18}\text{O}$ occurs during evaporation (Zimmermann et al. 1967), but transpiration is a non-fractionating process (Förstel 1982). Unlike $\delta^2\text{H}$ and $\delta^{18}\text{O}$, the accumulation of Cl^- in groundwater is a result of both evaporation and transpiration. A comparison between $\delta^{18}\text{O}$ and Cl^- in the 2009 pre-monsoon samples results in two different trends between $\delta^{18}\text{O}$ and Cl^- (Fig. S3). The lower slope is the regression line of the open well locations that suggests both an accumulation in Cl^- and enrichment in $\delta^{18}\text{O}$ due to evaporation, whereas the points that fall along the steeper slope indicated by the dashed line are likely to be dominated more by transpiration losses of water. One possible explanation for the dominance of transpiration losses in the deeper well and borehole samples is that the deeper water is older and representative of transpiration of native vegetation. The evolution of two distinct linear trends between $\delta^{18}\text{O}$ and Cl^- has been observed in a previous study that tracked the relative changes of H_2O and Cl^- in soil water, irrigation water, and groundwater during irrigation (van den Akker et al. 2011). It was found that

fractionation of water during evaporation in irrigation water was small (0-5 %) in comparison to the accumulation of Cl^- concentrations in soil water (23-117 %) due to transpiration. It is important to note that the well locations that fall along the transpiration trajectory are sites that are situated on high-density farms and near the Gomti River (Fig. S3), which are more likely to be influenced by high rates of groundwater recycling after the monsoon either due to irrigation return flow and/or lateral groundwater flow. High rates of groundwater recycling would increase the susceptibility for water losses from transpiration during irrigation.

Fig. S3 Cl^- concentrations and $\delta^{18}\text{O}$ in the 2009 pre-monsoon groundwater samples. The total depth of each well and borehole is shaded, such that the black symbols indicate deeper wells and boreholes, and the light grey symbols the more shallow.



3. Permutation test methodology

A permutation test was conducted to test the first hypothesis, that S_y varies between well locations. In order to test the null hypothesis that S_y is homogenous in all the wells across the watershed the following model was constructed:

$$R_{\text{CMB}(x,t)} = S_y Dh_{(x,t)} + e_{(x,t)} \quad (\text{S1})$$

where R_{CMB} is the recharge that would be estimated from the CMB method at each sample site (x) within a given year (t) , Dh is the change in water-table height, and e is the error. The alternative hypothesis is that S_y for each sample site has its own $S_{y(x)}$, such that the model can be:

$$R_{\text{CMB}(x,t)} = S_{y(x)} Dh_{(x,t)} + e_{(x,t)} \quad (\text{S2})$$

The S_y for the null hypothesis and $S_{y(x)}$ for the alternative hypothesis were estimated by minimizing the sum of square errors. Under the null hypothesis, this is the least-squares estimator for the regression with no intercept, and under the alternative hypothesis the same estimator is fit separately for each location. The S_y least squares estimate $(\hat{S}_{y(x)})$ at each location is determined by minimizing the square error of the alternative hypothesis model in Eqn (S1), such that the derivative of the resultant polynomial is equated to zero in Eqn (S2) and solves for $(\hat{S}_{y(x)})$ in Eqn (S3).

$$e_{(x,t)} = \sum \left(R_{\text{CMB}(x,t)} - \hat{S}_{y(x)} Dh_{(x,t)} \right)^2 \quad (\text{S3})$$

$$\frac{\partial}{\partial S_y} = \sum \left[\left(R_{\text{CMB}(x,t)} \right)^2 - 2R_{\text{CMB}(x,t)} \hat{S}_{y(x)} Dh_{(x,t)} + \left(\hat{S}_{y(x)} Dh_{(x,t)} \right)^2 \right] \equiv 0 \quad (\text{S4})$$

$$\hat{S}_{y(x)} = \frac{\sum \left(R_{\text{CMB}(x,t)} Dh_{(x,t)} \right)}{\sum \left(Dh_{(x,t)} \right)^2} \quad (\text{S5})$$

The test statistic (T_{obs}) for the sum of squared errors that results from fitting the model under the alternative hypothesis in Eqn (S2) is:

$$T_{\text{obs}} = \sum \left(e_{(x,t)} \right)^2 = \sum \left(R_{\text{CMB}(x,t)} - \hat{S}_{y(x)} Dh_{(x,t)} \right)^2 \quad (\text{S6})$$

where the least squares estimate of specific yield ($\hat{S}_y(x)$) and paired observed values for $R_{\text{CMB}(x,t)}$ and $Dh_{(x,t)}$ are utilized, such that paired values for each year are summed within a given location. The sum of squares that results from assuming the same S_y for the entire watershed in the null hypothesis (T_{null}) is:

$$T_{\text{null}} = \sum \left(R_{\text{CMB}(x,t)} - S_y Dh_{(x,t)} \right)^2 \quad (\text{S7})$$

The sum of squared errors for the null hypothesis (T_{null}) will always be larger than the sum of squared errors for the alternative hypothesis (T_{obs}). In order to decipher whether the T_{null} is statistically larger than the T_{obs} , a distribution of T_{obs} under the null hypothesis was created using paired observed values for $R_{\text{CMB}(x,t)}$ and $Dh_{(x,t)}$ between locations within a given year. A null distribution was created by perturbing the dataset and computing 10,000 T_{obs} by using various combinations of paired observed $R_{\text{CMB}(x,t)}$ and $Dh_{(x,t)}$ data between different locations within a given year.

The test statistic from the alternative hypothesis was statistically significant within the 95 % confidence interval, such that the null hypothesis was rejected; S_y values are indeed different across each of the well sites. It is sensible to assume that inter-annual changes in S_y at a specific location would be negligible, since S_y values are an intrinsic quantitative representation of the fraction of available pore space for groundwater within an unconfined aquifer. This suggests that the sum of square errors for the test statistic is a reflection of any uncertainty that exists with the empirical data collection.

It is generally assumed that S_y varies with depth and remains more homogenous laterally, particularly in fractured hard-rock aquifers that are generally characterized as having distinct layers throughout the weathering profile (Maréchal et al. 2004). The Gangeshwar watershed is part of the larger Precambrian Crystalline Province (Singhal and Gupta 2010), present in half of central and southern India, and is comprised of highly fractured basement. The geology in the Gangeshwar is likely to be similar to that described in the Maheshwaram watershed of South India, where 1) a layer of saprolite, 2) a fissured layer, and 3) a fresh basement, are present from the top down.

1) The saprolite layer (or regolith) is up to a few tens of meters thick and constitutes the unconsolidated weathered mantle that is derived from prolonged in situ decomposition of bedrock. The saprolite layer is characterized by a high porosity and low permeability due to the clay-sand composition.

2) The upper fissured layer (weathered fractured layer) is the most productive part of the aquifer (Houston and Lewis 1988; Taylor and Howard 2000; Maréchal et al. 2004) and predominantly characterized by dense horizontal fissures in the first tens of meters near the base of the saprolite layer (Maréchal et al. 2003) that decrease with depth (Maréchal et al. 2004). Horizontal features tend to be better connected and as a result are more permeable than sub-vertical fracture sets, although it is also possible that layers and lenses of weathered material can exist as secondary sedimentary deposits within the regolith. The presence of fissures is more a consequence of weathering than tectonic processes (Maréchal et al. 2003).

3) Fresh basement is locally permeable and fissures that are present are derived from tectonic processes.

Although fractured hard rock systems are considered to be homogeneous horizontal layers (Maréchal et al. 2004), it is important to consider that topographic differences and the total depth at each hand-dug open well location will intercept different layers of the aquifer system. For example, it has been observed in the Gangeshwar watershed that horizontal and sub-vertical fissures are more common in the western part of the watershed as opposed to the flatter east. This presents a challenge when trying to assign a S_y in fractured hard rock, as it not only varies horizontally based on topographic differences but also vertically due to the weathering profile.

References

- Choubisa SL (2001) Endemic fluorosis in southern Rajasthan, India. *Fluoride* 34:61–70.
- Edmunds W, Fellman E, Goni I, Prudhomme C (2002) Spatial and temporal distribution of groundwater recharge in northern Nigeria. *Hydrogeology Journal* 10:205–215. doi: 10.1007/s10040-001-0179-z
- Edmunds WM, Smedley PL (2013) Fluoride in natural waters. In: *Essentials of Medical Geology*. *Essentials of medical geology*, pp 311–336
- Förstel H (1982) $^{18}\text{O}/^{16}\text{O}$ ratio of water in plants and their environment. In: Schmidt HL, Förstel H, Heinzinger K (eds) *Stable Isotopes*. Elsevier, Amsterdam, The Netherlands, pp 503–516
- Fritz P, Frapre SK (1987) *Saline water and gases in crystalline rocks*. Department of Earth Sciences
- Hem JD (1985) *Study and Interpretation of the Chemical Characteristics of Natural Water*. USGS, Alexandria
- Houston J, Lewis RT (1988) The Victoria Province drought relief project, II. Borehole yield relationships. *Ground Water* 26:418–426.
- Kamineni DC (1987) Halogen minerals in plutonic rocks: a possible source of chlorine in saline groundwater in the Canadian Shield. *Geological Association of Canada Special Paper* 33:69–79.
- Maréchal J-C, Wyns R, Lachassagne P, et al (2003) Vertical anisotropy of hydraulic conductivity in fissured

layer of hard-rock aquifers due to the geological structure of weathering profiles. *Comptes Rendus Géoscience* 335:451–460. doi: 10.1016/S1631-0713(03)00082-8

Maréchal JC, DEWANDEL B, Subrahmanyam K (2004) Use of hydraulic tests at different scales to characterize fracture network properties in the weathered-fractured layer of a hard rock aquifer. *Water Resources Research* 40:n/a–n/a. doi: 10.1029/2004WR003137

Singhal BBS, Gupta RP (2010) *Applied Hydrogeology of Fractured Rocks*. Springer Science & Business Media

Taylor R, Howard K (2000) A tectono-geomorphic model of the hydrogeology of deeply weathered crystalline rock: evidence from Uganda. *Hydrogeology Journal* 8:279–294.

van den Akker J, Simmons CT, Hutson JL (2011) Salinity Effects from Evaporation and Transpiration under Flood Irrigation. *J Irrig Drain Eng* 137:754–764. doi: 10.1061/(ASCE)IR.1943-4774.0000364

Zimmermann U, Münnich KO, Roether W (1967) Downward movement of soil moisture traced by means of hydrogen isotopes. *Geophys Monogr Ser* 11:28–36. doi: 10.1029/GM011p0028

Table S1 Groundwater sample results, June 2009 (Pre-monsoon)

Water Point ID	$\delta^{18}\text{O}$	$\delta^2\text{H}$	Chloride (mg/L)	Nitrate (mg/L)	Sulphate (mg/L)	Fluoride (mg/L)
1	-4.3	-31.1	235.6	155.8	73.8	below detection
2	-6.4	-47.5	234.9	320.7	91.4	below detection
3	-4.4	-20.3	375.5	71.4	77.6	below detection
4	-5.0	-35.6	33.4	39.4	11.7	below detection
5	-4.4	-32.5	116.7	172.3	32.4	below detection
6	-5.1	-36.8	123.9	181.2	28.8	below detection
7	-5.9	-42.5	34.6	79.9	30.3	below detection
8	-5.9	-42.1	17.2	52.1	12.0	below detection
9	-5.6	-40.5	13.8	8.7	19.1	1.0
10	-2.2	-20.3	44.5	below detection	4.2	below detection
11	-5.4	-40.1	42.1	58.8	16.1	below detection
12	-4.5	-31.4	59.7	below detection	41.2	1.6
13	-3.3	-27.1	41.6	below detection	12.4	below detection
14	-4.7	-27.8	232.2	93.7	45.2	below detection
15	-3.4	-26.0	99.6	42.0	31.7	below detection
17	-6.1	-45.8	19.9	30.4	13.5	below detection
18	-5.9	-44.4	45.8	10.7	17.8	below detection
19	0.5	-3.0	126.2	below detection	below detection	below detection
20	-6.5	-48.7	61.7	75.5	32.5	below detection
21	-6.3	-46.5	39.0	43.9	26.1	below detection
22	-6.7	-48.2	19.9	23.0	15.2	below detection
26	-4.2	-29.5	28.2	28.7	8.4	below detection

27	-5.1	-35.9	18.5	32.6	11.9	below detection
28	-4.8	-32.4	29.2	38.3	11.6	below detection
29	-0.7	-10.9	20.7	0.6	6.6	below detection
30	no data	no data	12.0	below detection	1.5	below detection
33	-5.1	-39.0	23.0	below detection	7.1	below detection
34	-5.2	-38.7	22.5	39.4	15.3	below detection
35	-5.5	-41.7	21.3	35.0	15.7	below detection
36	-5.4	-39.0	30.6	46.3	20.7	below detection
37	-4.8	-36.0	26.7	15.2	20.7	below detection
38	-5.3	-37.1	15.3	12.9	13.7	below detection
39	no data	no data	22.1	6.0	13.2	1.4
40	-5.7	-40.0	34.0	94.6	21.4	below detection
41	-5.1	-36.9	39.3	83.5	21.9	below detection
42	-5.9	-44.1	25.4	129.9	25.9	below detection
43	-4.6	-34.3	154.9	102.4	59.1	below detection
44	-4.4	-31.8	82.7	197.1	29.9	below detection
45	-4.2	-32.2	30.1	19.5	11.6	below detection
46	-5.3	-39.9	59.0	155.5	20.0	below detection
47	-5.4	-38.8	65.9	87.2	22.9	below detection
48	-5.2	-36.4	33.4	below detection	10.5	below detection
49	-4.4	-34.2	29.5	below detection	11.9	below detection
50	no data	no data	26.7	7.9	11.0	0.5
51	-3.7	-30.4	17.4	below detection	8.8	below detection
52	-3.7	-34.1	51.2	below detection	12.4	1.5
53	-4.7	-35.7	38.9	below detection	5.5	below detection

54	-5.7	-44.4	44.3	160.1	24.3	below detection
55	-5.8	-45.7	82.1	27.9	18.7	below detection
56	-2.4	-26.5	89.5	below detection	13.1	below detection
57	-5.9	-43.2	115.6	174.0	42.6	below detection
58	-5.2	-43.5	96.5	70.1	31.4	below detection
59	-4.6	-36.6	62.0	below detection	13.2	below detection
60	-4.9	-36.9	40.0	6.6	10.6	below detection
61	-4.1	-35.8	104.1	47.1	15.9	below detection
62	-4.6	-32.9	25.8	18.2	14.5	below detection
63	-4.2	-37.0	45.1	below detection	20.7	below detection
65	-2.1	-23.4	117.9	2.3	17.6	below detection
66	-6.1	-45.5	25.7	16.9	14.1	below detection
67	-5.5	-39.9	21.2	20.2	8.6	below detection
68	-5.0	-38.9	191.0	below detection	34.7	below detection
70	-4.8	-35.8	233.0	115.0	250.6	below detection
71	-4.1	-32.2	133.3	141.2	54.7	below detection
72	-2.8	-25.5	28.0	1.6	4.3	below detection
73	-4.9	-36.3	29.1	50.3	10.8	below detection
74	-3.9	-30.3	21.2	6.1	9.2	below detection
75	-5.4	-39.6	27.4	14.6	8.5	below detection
77	-5.8	-39.8	12.3	23.3	10.7	below detection
78	-2.6	-18.4	25.0	1.3	3.4	below detection
79	-2.6	-24.9	37.7	below detection	10.8	1.9
80	-2.7	-26.1	43.3	1.9	11.1	below detection

81	-4.5	-32.6	86.5	133.2	10.7	below detection
82	-5.2	-38.1	39.1	28.2	11.4	below detection
83	-4.9	-34.3	20.3	52.5	8.4	below detection
84	-5.0	-38.7	19.0	below detection	7.4	below detection
85	-6.9	-49.4	19.2	12.5	13.7	below detection
86	no data	-42.9	40.8	49.7	19.3	below detection
87	-6.2	-44.2	23.5	below detection	15.2	below detection
88	-5.4	-39.6	29.8	8.7	17.8	below detection
89	-5.7	-38.3	13.7	18.2	8.8	below detection
90	-5.1	-41.0	28.1	9.5	16.6	below detection
91	-5.3	-37.3	28.4	9.3	16.2	below detection
92	-5.6	-45.1	19.0	37.0	15.4	below detection
93	-5.3	-37.3	34.7	23.0	24.6	below detection
94	-5.6	-40.3	34.0	36.0	22.2	below detection
95	-5.2	-37.9	46.5	27.3	30.5	below detection
96	-5.0	-36.8	96.6	20.9	37.4	below detection
97	-5.6	-42.9	103.5	5.6	24.8	below detection
98	-5.2	-40.0	151.6	32.6	39.5	below detection
99	-4.1	-31.2	535.3	below detection	86.5	below detection
100	-4.0	-32.3	84.8	39.2	29.1	below detection
101	-6.1	-41.8	437.3	9.5	63.9	below detection
106	-5.7	-41.8	25.8	39.4	18.1	below detection
107	-6.1	-46.9	31.4	50.8	25.1	below detection
108	-4.7	-35.6	76.2	5.1	25.1	below detection
109	-4.7	-35.8	47.9	39.6	30.0	0.4

Table S2 Groundwater sample results, January 2010 (Post-monsoon)

Water Point ID	Chloride (mg/L)	Nitrate (mg/L)	Sulphate (mg/L)	Fluoride (mg/L)
17	27.4	48.8	18.5	0.8
18	51.7	55.8	27.1	1.0
19	53.1	40.8	13.6	below detection
20	59.1	147.2	33.3	1.3
21	63.7	74.9	27.5	1.0
22	23.8	23.4	16.4	0.7
33	30.3	15.1	15.4	0.8
34	39.6	71.2	24.5	0.9
35	36.1	67.4	25.4	0.9
36	50.1	95.6	31.2	0.9
37	47.1	120.4	32.0	1.0
38	27.4	50.5	20.5	0.7
39	40.3	13.9	23.5	1.3
41	66.5	128.2	31.7	0.8
42	48.0	229.1	36.9	0.6
84	20.3	13.8	25.7	0.9
85	29.6	50.0	19.3	1.0
86	54.2	79.0	24.4	0.8
87	36.4	67.4	22.7	0.7
88	38.8	58.0	22.3	0.7
89	20.7	56.4	13.4	0.5
90	48.3	42.7	25.7	0.6
91	46.8	41.1	25.9	0.9
92	42.3	81.9	28.0	0.9
93	46.8	106.2	31.5	0.8
94	63.9	86.9	35.5	1.1
95	67.8	47.0	42.3	0.9
96	107.4	88.6	57.1	0.7
97	123.9	7.7	21.3	0.5
98	185.4	91.1	60.3	0.5
99	135.4	50.3	41.2	0.6
100	111.4	54.6	38.9	0.7
101	349.4	18.7	58.7	0.5
103	34.8	16.1	5.6	0.7
104	19.1	18.2	5.9	0.5
106	47.5	84.7	29.3	0.8
107	67.9	130.1	44.1	0.8
108	101.9	27.9	38.6	1.5
109	88.7	45.3	48.4	2.4

Table S3 Groundwater sample results, June 2010 (Pre-monsoon)

Water Point ID	Chloride (mg/L)	Nitrate (mg/L)	Sulphate (mg/L)	Fluoride (mg/L)
3	358.9	110.5	75.5	0.8
17	20.2	35.3	14.7	0.5
18	49.2	12.3	23.8	0.7
19	93.1	146.2	10.1	0.3
20	107.9	149.6	45.2	0.5
21	29.4	49.8	21.8	0.4
23	62.8	63.8	37.9	0.9
24	52.2	32.1	28.8	1.2
30	15.0	3.4	9.9	0.3
33	21.3	below detection	7.0	0.5
34	30.8	28.9	20.4	0.5
35	27.1	50.4	21.0	0.6
36	40.7	64.3	25.6	0.5
37	41.1	19.7	3.8	0.7
38	20.8	below detection	13.8	0.5
39	28.1	9.5	17.8	0.7
41	44.3	107.9	24.4	0.5
84	23.4	15.5	11.4	0.6
85	42.5	20.4	17.8	0.5
86	33.2	55.2	19.6	0.5
87	17.6	27.4	11.3	0.3
88	39.3	10.5	14.2	0.4
89	41.1	15.7	21.9	0.4
92	38.2	32.7	20.8	0.7
93	31.0	54.2	21.6	0.6
94	42.0	26.0	28.2	0.7
95	53.7	79.4	31.4	0.6
97	127.2	26.9	42.3	0.6
98	137.5	8.4	31.9	0.3
99	141.0	58.2	46.5	0.4
100	71.9	41.2	42.5	0.5
103	20.6	below detection	6.5	0.6
106	51.4	77.2	38.9	0.5
107	115.4	5.1	31.9	1.3
108	74.1	37.9	38.6	1.3
109	25.8	25.8	2.5	0.5

Table S4 Groundwater sample results, April 2011 (Pre-monsoon)

Water Point ID	Chloride (mg/L)	Nitrate (mg/L)	Sulphate (mg/L)	Fluoride (mg/L)
1	303.8	335.9	96.4	0.2
3	483.0	124.6	90.5	0.6
4	50.4	68.1	19.2	0.6
5	273.3	343.7	72.3	0.3
7	37.2	50.8	30.9	0.5
10	78.6	44.1	21.4	0.8
13	70.9	27.9	11.0	0.3
14	327.7	131.2	54.8	0.7
16	26.9	3.6	6.3	0.5
17	21.4	42.9	13.3	0.6
18	50.7	42.1	24.7	0.7
20	93.7	79.7	58.7	0.8
21	54.7	34.3	28.2	0.6
22	25.0	9.1	13.4	0.5
23	75.7	99.2	38.7	0.6
25	20.1	13.9	14.0	0.5
28	42.3	no data	14.1	0.7
29	27.6	21.4	9.8	0.7
30	22.9	no data	12.1	0.4
31	17.2	23.2	13.2	0.8
32	54.9	49.9	21.9	0.8
34	35.9	74.6	23.9	0.6
36	50.1	95.6	30.5	0.6
37	47.2	165.5	32.7	0.6
41	56.8	134.8	29.7	0.6
47	114.5	194.0	40.0	0.5
50	58.9	43.1	18.0	0.6
55	141.3	84.6	26.1	0.7
56	97.5	43.4	18.4	0.5
57	178.9	276.2	61.1	0.4
60	43.3	1.6	15.6	0.5
61	180.6	111.0	21.0	0.7
62	29.0	51.1	17.8	1.0
64	171.6	124.8	45.6	0.5
68	69.9	25.1	26.9	0.3
69	72.0	30.1	92.7	below detection
72	39.7	1.9	10.0	0.5
76	62.7	5.6	15.7	0.6
81	152.1	215.5	13.3	0.6
82	28.0	35.8	11.7	0.6
83	17.9	75.1	12.8	0.8
89	17.3	25.9	10.9	0.4
91	38.4	7.6	21.0	0.6
92	35.0	55.8	26.0	0.6

93	51.3	50.3	27.8	0.6
97	53.1	2.2	11.9	0.4
98	146.0	72.7	57.8	0.4
99	62.3	no data	10.5	0.6
100	71.1	44.8	31.4	0.5
102	70.2	69.4	37.5	0.6
105	83.3	35.5	35.0	0.5
110	54.9	93.0	36.1	0.6
111	56.4	3.4	8.5	0.9